

Lawrence Berkeley National Laboratory

LBL Publications

Title

Model-based data center cooling controls comparative co-design

Permalink

<https://escholarship.org/uc/item/10r2g9vw>

Journal

Science and Technology for the Built Environment, 30(4)

ISSN

2374-4731

Authors

Grahovac, Milica

Ehrlich, Paul

Hu, Jianjun

et al.

Publication Date

2024-04-20

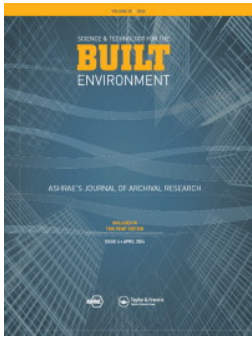
DOI

10.1080/23744731.2023.2276011

Copyright Information

This work is made available under the terms of a Creative Commons Attribution License, available at <https://creativecommons.org/licenses/by/4.0/>

Peer reviewed



Model-based data center cooling controls comparative co-design

Milica Grahovac, Paul Ehrlich, Jianjun Hu & Michael Wetter

To cite this article: Milica Grahovac, Paul Ehrlich, Jianjun Hu & Michael Wetter (2024) Model-based data center cooling controls comparative co-design, Science and Technology for the Built Environment, 30:4, 394-414, DOI: [10.1080/23744731.2023.2276011](https://doi.org/10.1080/23744731.2023.2276011)

To link to this article: <https://doi.org/10.1080/23744731.2023.2276011>




This work was authored as part of the Contributor's official duties as an Employee of the United States Government and is therefore a work of the United States Government. In accordance with 17 USC. 105, no copyright protection is available for such works under US Law.



Published online: 11 Dec 2023.




[Submit your article to this journal](#) 



Article views: 692



[View related articles](#) 



[View Crossmark data](#) 

Model-based data center cooling controls comparative co-design

MILICA GRAHOVAC^{1*}, PAUL EHRLICH², JIANJUN HU¹ AND MICHAEL WETTER¹

¹Lawrence Berkeley National Laboratory, 1 Cyclotron Road, Berkeley, CA, USA

²Building Intelligence Group, Afton, MN, USA

This article presents a comparative simulation-based control logic design process. It uses the Control Description Language (CDL) and the ASHRAE Guideline 36 high-performing building control sequences with the Modelica Buildings Library (MBL) to demonstrate a comparative analysis of two control designs for a data center chilled water plant. Details include a description of the closed-loop plant and control design methodology, including sizing and parameterization, base and alternative (Guideline 36) control logic with software implementation structure, and outline of the simulation experimentation process. The selected control designs are paired with comparable chilled water plant configurations. The models include a chiller, a water-side economizer, and an evaporative cooling tower. The plant provides cooling at 27°C zone supply air temperature to a data center in Sacramento, CA. The comparative simulation results examined the impacts of a selected control logic detail, and present an example model-based design application. Overall, the simulation results showed a 25% annual and a 18% summer energy use reduction for alternative controls. This shows that simulation-based control logic design performance evaluation can improve energy efficiency and resilience aspects of system controls at large.

Introduction

Standardization of high-performing building control sequences enables implementation of control sequences in customizable software packages. Coupled with existing software libraries of system and component models, the emergence of control sequence libraries opens up new and exciting space in model-based load, plant, and controls co-design. The OpenBuildingControl (OBC) project¹ paved a way to broader application of control software libraries, as it, among other things, implemented the ASHRAE Guideline 36 (G36) (ASHRAE 2021) high-performing sequences in the Modelica Buildings Library (Wetter et al. 2014), defined the Control

Description Language (CDL) (Wetter, Grahovac, et al. 2018), and invented the digital controls delivery process (Wetter et al. 2022). CDL is currently being standardized through the ASHRAE Proposed Standard 231 P.²

OBC tools and processes, including the implementation of CDL, were first demonstrated in a simulation case study (Wetter, Grahovac, et al. 2018) that compared a G36-based secondary multizone variable air volume HVAC controller with an alternative ASHRAE published control sequence from 2006. As a load, the study used a floor of the Department of Energy (DOE) prototypical large office building. The study produced dynamic simulation models capable of detailed evaluation of the controller implementations and the consequential comparative energy use savings. Zhang et al. (2020) presented a comparative model-based study that also evaluated the energy savings of G36 controls of the air side of a single-zone variable air volume system (secondary system). While both studies perform a comparative model-based control design, they are oriented toward the secondary system, rather than toward the water side (primary system). The OBC project introduced first practical forms of control sequence functionality verification, as presented in Wetter, Hu, et al. (2018). In the domain of sequence comparison, there exists a framework for benchmarking of building HVAC control algorithms called BOPTTEST (Building optimization testing framework, described in Blum et al. [2021]). BOPTTEST is broader than our needs for this article, and it focuses on buildings rather than data centers, in terms of both

Received May 7, 2023; accepted September 23, 2023

Milica Grahovac, PhD, Associate Member ASHRAE, is a Energy/Environmental Policy Researcher III. **Paul Ehrlich, PE, Full Member ASHRAE**, is a Founder and President. **Jianjun Hu, PhD**, is a Technology Researcher III. **Michael Wetter, PhD, Full Member ASHRAE**, is a Computational Senior Scientist/Engineer.

*Corresponding author e-mail: mgrahovac@lbl.gov

This is an Open Access article that has been identified as being free of known restrictions under copyright law, including all related and neighbouring rights (<https://creativecommons.org/publicdomain/mark/1.0/>). You can copy, modify, distribute and perform the work, even for commercial purposes, all without asking permission. The terms on which this article has been published allow the posting of the Accepted Manuscript in a repository by the author(s) or with their consent.

comparison metrics and models. Fan et al. (2021) provided model-based comparative control designs for chiller plants with a water-side economizer (WSE) in data centers, evaluating their energy performance across multiple control scenarios. The sequences are developed for an array of data center chiller plant configurations that are implemented as open-source models in Modelica and not in CDL.

ASHRAE Guideline 36 2021 specifies sequences for chiller and boiler plants. Although the guideline does not address data center cooling applications specifically, many of the control sequences can be applied to such systems. We structured, modularized, and generalized the software implementation of the control sequences in the Modelica Buildings Library (MBL). This allows for practical sequence customizations beyond those explicitly outlined in the ASHRAE guideline.

As we were writing this article, we were not able to identify any previously published work that utilizes or evaluates G36-based chiller plant sequences implemented in CDL. To start addressing the gap, this article describes the first comparative model-based co-design and simulation performance evaluation study for a G36-based controller implemented in CDL applied on a data center chiller plant. The approach can further be utilized to develop high-level-of-detail custom and innovative plant and control co-designs, including further applications of the primary system G36-based controllers.

In this article, we introduce and describe, supported by an example, a model-based comparative controls design process. We demonstrate the application of the design process on a data center chilled water plant including a water-side economizer located in Sacramento, CA. The article provides detailed insight and incorporates and builds upon the data center chiller plant case study first presented in Grahovac et al. (2022). There we compared the closed-loop system performance of two different chiller plant controllers, one based on ASHRAE Guideline 36 and implemented in CDL and the other derived from the one applied in Wetter et al. (2014). Compared to Grahovac et al. (2022), this article expands on the following items:

- We describe the simulation-based comparative design process.
- We detail the parameterization and sizing procedure, including its software realization; introduce the structural layers and hierarchy of the control sequence software library and the controller implementations; and further elaborate on the model and controls implementation.
- We expand the data center zone supply air temperature set-point sensitivity analysis; present the sensitivity to a selected small difference in control logic; and provide deeper insights regarding the alternative and broader uses of close-coupled simulation models as a design aid, in this case, to identify conditions for chiller-less cooling plant design.
- We add comments on decentralized data center resilience as an integral part of the future power grid.

In the example design study, we used two controller designs—a *base case* and an *alternative design*. In the base case model, we applied a controller similar to that presented in Wetter et al. (2014), with a few upgrades introduced to the condenser water-side hydronic configuration and control implementation structure. The major aspects of the base case

controls are the chilled water reset and the utilization of three smaller condenser water pumps in a custom hydronic configuration to ensure minimal chiller lift. We designed the alternative controller for this study primarily based on our adaptation of certain control algorithms from ASHRAE Guideline 36. In addition to the chilled water reset, the alternative controller applies the condenser water reset and relies on the original and simpler condenser water-side hydronic configuration from Wetter et al. (2014).

In our study of the simulation results, we saw that the water-side economizer is nearly fully capable of satisfying the load, without use of the chiller. This prompted us to investigate the plant design's ability to meet the load throughout the year in a chiller-free operation. We introduced a novel simulation-based configuration and sizing design method to help identify a set of loading and climate conditions leading to chiller redundancy. In the main set of design parameters, the system redundancy is treated similarly in the two cases, with the chiller nominal power being slightly lower than the nominal load, yet the chiller is operated at high coefficients of performance (COP) due to the relatively high supply air temperature set-point. Effectively, this brings the designs close to an $N+1$ redundancy of the cooling source, contributing toward fulfilling the Tier II rating requirements, per data center Tier classification explained in Velimirovic (2021). In real systems the $N+1$ redundancy would also include one redundant pump and fan for each one existing in the system.

The article explores, through a detailed example, some of the challenges of model-based design process for HVAC applications. Future design automation tools have a complex task of allowing for design customization while providing a high level of automation in both system and building design.

The article has the following structure: “Simulation-based comparative controls design process” outlines the comparative controls design process. “System and controls design methodology” describes the system and control design methodology, walks through the system configuration of chilled water plant designs, details the base and alternative controllers, and presents the sizing and the parameterization assumptions. “Software implementation” presents the model implementation, the software libraries of high-performing control sequences, the controller hierarchy and parameterization, and the experimentation environment. “Results” provides the comparative annual and summer performance results, investigates the sensitivity to the data center zone supply air temperature set-point, and presents a generic method useful in weather-dependent co-design. Finally, “Conclusion” discusses the findings.

Simulation-based comparative controls design process

With the increase in complexity of building control sequences emerged the need for a simulation-based plant and control design process. Higher complexity arising from the desire to conserve energy inherently increases the error probability. To mitigate some of the risks associated with the site application of high-performing complex control algorithms,

we conducted a comparative control co-design process that can be embedded into any broader simulation-supported design, testing, and verification framework, such as the OBC project's digital control delivery framework. The steps of the plant and controls design process are:

1. Design the chiller plant system based on the cooling load. To simplify the comparison, we assumed that the plant needs to meet a constant cooling load.
2. Implement the base and the alternative control logic. The choice of the base and the alternative control logic design may depend on system complexity, climate, cost constraints, energy standards, availability of standardized control libraries, and so on.
3. Refine the chiller plant configuration based on the chosen control systems. This step may be skipped if both control designs can be applied on identical plant configuration.
4. Implement the system model using Modelica libraries. We created two model implementations, one for the base and the other for the alternative system configuration.
5. Implement the base control logic using MBL packages not limited to the use of CDL.
6. Implement the alternative control systems using the ASHRAE G36-based control logic packages implemented in CDL and located under MBL's OBC package. Ideally the user would choose both base and alternative control designs from a library of standardized sequences, depending on the availability.
7. Connect the control systems to the plant system and configure them.
8. Perform simulation experiments to investigate the sizing, the configuration, and the controls performance of the design cases, for a chosen weather year and location. In this step, the modeler or designer has the ability to evaluate any aspect of the plant performance.
9. Utilize the annual simulation result time-series, to discuss, compare, and present various aspects of the controls performance.

System and controls design methodology

This section details the base and alternative chiller plant configuration and their respective control system configurations, and describes key assumptions regarding the plant component sizing and controller parameterization.

Demonstrating how to use the model to design a robust controller is beyond the scope of this work. However, we refer interested readers to the following reports, which all used a Modelica model to design a robust controller: Wetter (2009) designed a PI (proportional-integral) controller with gain scheduling in the frequency domain, Wetter and Hu (2019) co-designed an HVAC hydronic configuration and associated controls after demonstrating that the baseline controller was unstable, and Bortoff et al. (2022) developed an H-infinity loop shaped model predictive controller.

The base model leverages algorithms primarily developed by Taylor Engineers³ as previously applied in the example

presented in Wetter et al. (2014). The alternative model stems from sequences specified through ASHRAE Guideline 36 with, to the best of our knowledge, no prior applications in system simulation.

Three fluid loops define the major pattern found in both chilled water plant system configurations: the air loop, and the hydronic loops: the chilled water (CHW) loop and the condenser water (CW) loop. The sizing of main system components in all three fluid loops remains either the same or, in case of any configuration differences, comparable across the two cases.

Both systems are, for simplicity, serving an identical and constant data center cooling load. We model the data center zone idealized by adding its emitted heat to the return air (using a first-order delay).

Chilled water plant system configuration

In both configurations the chiller plant comprises a chiller and a WSE, connected in series on the CHW side and in parallel on the CW side, CHW and CW pumps, and a single-cell cooling tower.

Each plant configuration is matched with a set of chiller plant control sequences, called *base* and *alternative controllers*. The plants have different hydronic configurations on the CW side and require a somewhat different set of sensors.

Figures 1 and 2 present the schematics of the base and the alternative plant and control models, respectively. The figures lay out the main system components and the hydronic configuration, including the controller instrumentation. Sections on the right side of each figure lay out the control approach and provide most important details of the control algorithm, such as state charts and control diagrams for selected variables. The opaque-transparent color coding utilized for set-points and instrumentation is such that any opaque filled thermostat, flow meter, or set-point applies in the alternative case, transparent filled applies to the base case, and any half-opaque element is present in both configurations. This approach helps observe the differences between the instrumentation requirements among the two cases.

The plant configuration schematics show that the first fluid loop, the air loop, remains the same in both configurations: A supply air fan circulates air through a cooling coil to supply cooling to the data center room. The control objective is to maintain a constant zone supply air temperature $T_{z,s}$, as measured by a sensor located between the air supply fan and the data center zone.

The hydronic configuration of the CHW loop is also identical among the two cases. It consists of a CHW pump that circulates water from the cooling coil through the WSE. If additional cooling capacity is required, the chiller is enabled and valves open to allow for the chiller to receive water from the WSE in series. In both designs we measure the chilled water return temperature $T_{chw,r}$ and its value downstream of WSE, $T_{chw,r,d}$. The alternative configuration places additional two sensors in the CHW loop, to measure the

Legend

- Chiller
 - Cooling tower with a fan
 - Heat exchanger
 - Fan
 - Pump
 - Variable Speed
 - Valve Automatically controlled
 - Thermostat
 - Flow meter
 - Setpoint
- Color scheme**
- Any thermostat, flow meter, or setpoint
 - Filled - alternative controller
 - Filled and empty - both
 - Empty - base-case controller
- Connectors**
- Plant piping
 - Sensor to logic
 - Logic to actuator
 - Logic to logic

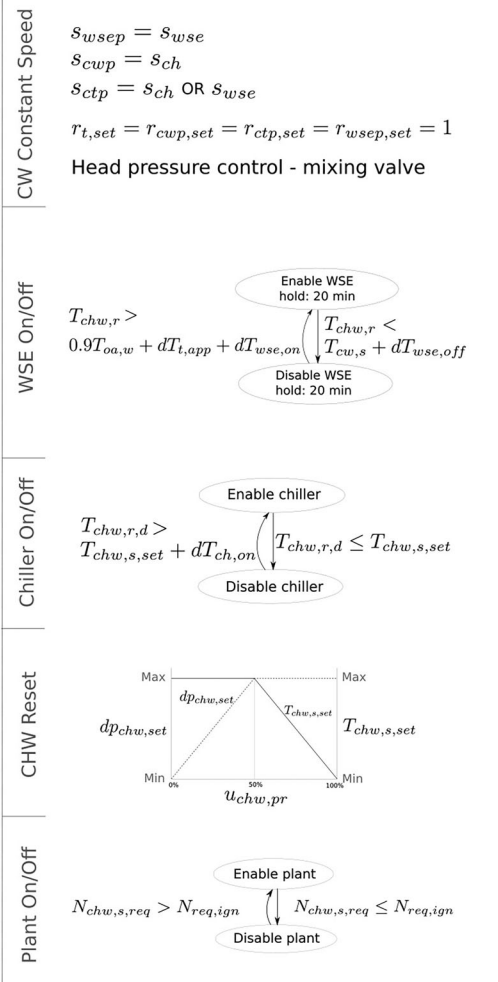
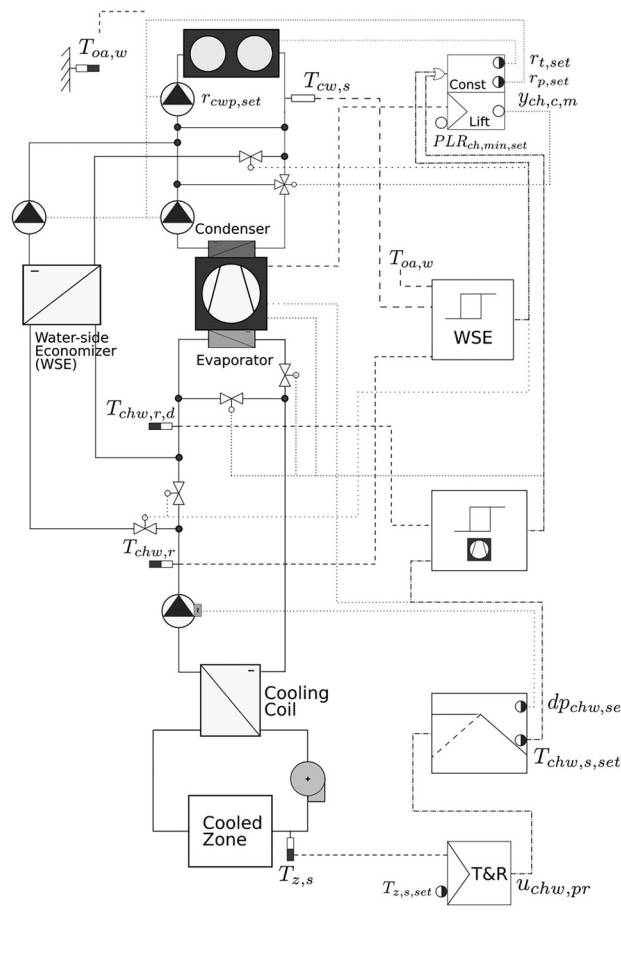


Fig. 1. Base case data center chilled water plant and controls design, left to right: plant diagram, control diagrams, and control sections with state charts.

chilled water supply temperature $T_{chw,s}$ and its volume flow $\dot{V}_{chw,s}$. If the chiller is disabled while the plant operates, the chiller bypass valve in both configurations closes to prevent flow and therefore pressure drop through the evaporator.

Lastly, the hydronic configuration of the CW loop differs between the two cases. The base case contains three smaller CW pumps, one each for the chiller condenser, the WSE, and cooling tower loops. The alternative case, however, uses the same configuration as in Wetter et al. (2014), which has a single CW pump with isolation valves for the chiller and the WSE. Both cases require an outdoor air wet-bulb temperature $T_{oa,w}$ sensor. The base case, in addition, requires a CW supply temperature $T_{cw,s}$ sensor, while the alternative case uses a CW return temperature $T_{cw,r}$ and a dry-bulb outdoor temperature T_{oa} sensor. Both CW-loop configurations guard the chiller from operating under low temperature lifts.

To summarize the instrumentation needs, the base configuration requires five temperature sensors, while the alternative requires a total of seven sensors. The modifications in the alternative case include two sensors in the CHW loop to allow for heat flow rate measurement, and different

placement of the CW-loop temperature sensor. We assumed no additional instrumentation is needed to measure T_{oa} in addition to the wet-bulb temperature $T_{oa,w}$, as the wet-bulb sensors usually also report dry-bulb temperature and humidity.

Base and alternative controllers

We set the supply air fan to operate at constant speed in both configurations due to the constant cooling load.

We sectioned each of the controllers into five control sections, as illustrated on the right-hand side of Figures 1 and 2. The control sections are, from the bottom to the top of the images, plant enablers, CHW reset, chiller enablers and staging logic, WSE enablers, and CW-loop control.

The *plant on/off* control section is identical in both design cases. A trim and respond logic generates a number of requests based on comparing the measured zone supply air temperature $T_{z,s}$ with its set-point. The logic can ignore a user configurable number of requests, and once enough requests are being generated, the plant is switched on. A real

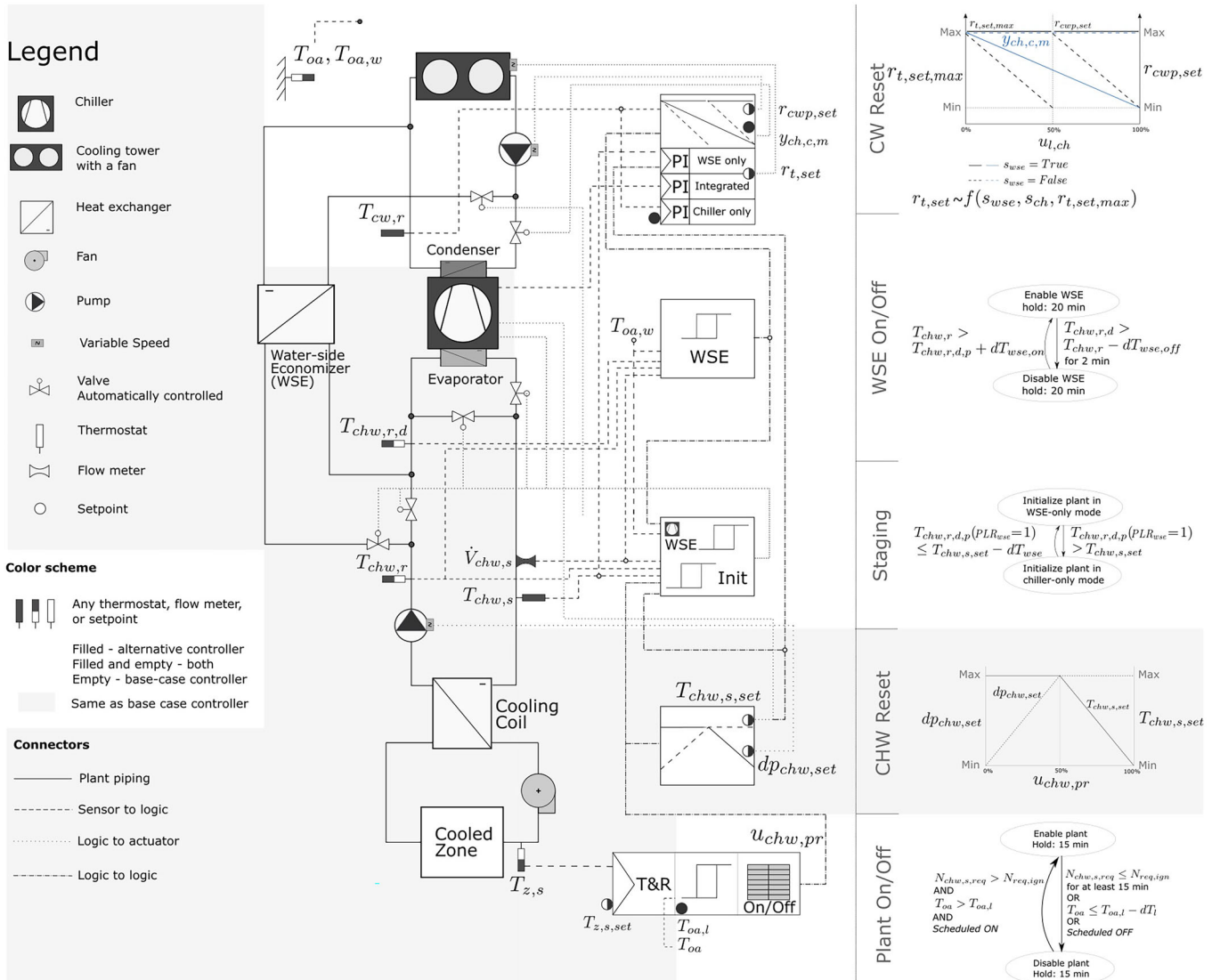


Fig. 2. Alternative case data center chilled water plant and controls design, left to right: plant diagram, control diagrams, and control sections with state charts. Transparent background highlights the differences compared to the base case controller illustrated in Figure 1.

plant, unlike a simulated one, would likely have an additional layer of manual override built into the hierarchy of the logic.

The *CHW reset* is utilized in both cases. When the zone requires more cooling, a control signal based on the number of cooling requests $u_{chw,pr}$ acts in two ways. First it increases the DP set-point of the CHW pump $dp_{chw,set}$ up to its maximum. Further increase in cooling demand decreases the CHW temperature set-point, $T_{chw,s,set}$. Effectively, the control intent is to gain more cooling capacity through first increasing the flow, followed by decreasing the temperature difference in the CHW loop.

The following two sections discuss the logic used to enable or disable the chiller and the WSE. The base case handles the chiller enabling independently from the WSE enabling logic, while the alternative controller uses the

ASHRAE G36 2021 staging logic, which integrates the WSE as one of the plant stages and provides separate logic to select the initial plant stage. In addition, the alternative controller uses the ASHRAE G36-based WSE enabling controller.

The *chiller on/off* algorithm of the base design is shown in the dedicated state chart on Figure 1. The chiller is enabled when the temperature measured downstream of the WSE in the CHW-loop $T_{chw,r,d}$ is sufficiently above the chilled water supply temperature set-point $T_{chw,s,set}$. If the chilled water return temperature downstream of WSE $T_{chw,r,d}$ drops to the chilled water supply temperature set-point $T_{chw,s,set}$, the chiller is switched off. The plant, however, may still continue to operate in a WSE-only mode. The decision to enable the WSE is made based on the outdoor air wet-bulb temperature $T_{oa,w}$, design cooling tower

approach $dT_{t,app}$, and a given temperature offset $dT_{wse,on}$. The WSE is disabled if the CHW return temperature $T_{chw,r}$ is below the CW supply temperature $T_{cw,s}$ plus a dead-band $dT_{wse,off}$.

To operate the chiller, the alternative controller uses the chiller *staging* logic. We used a generic n -chiller staging controller, implemented based on ASHRAE G36, and parameterized it for one chiller and one WSE. The initial stage selection logic makes use of the prediction of the temperature downstream of the WSE $T_{chw,r,d}$, to select whether the plant initiates in the WSE-only or in the chiller-only mode. The initialization state chart is provided in Figure 2 in the staging section. After selecting the initial stage, the logic continuously determines the chiller and the WSE status. A WSE control state chart in Figure 2 shows that the WSE is enabled if the WSE is expected to achieve a sufficient decrease in the CHW temperature across the WSE. That is, if the $T_{chw,r}$ is sufficiently above the downstream temperature prediction $T_{chw,r,d,p}$, the WSE is enabled. The predicted temperature $T_{chw,r,d,p}$ is calculated using the outdoor air wet-bulb temperature $T_{oa,w}$, the CHW volume flow measurement, and a plant-specific WSE self-tuning parameter. The tuning parameter is learned, in real or simulated time, based on the duration of the WSE states and the cooling tower fan speed. Once enabled, the WSE gets disabled if the temperature decrease across the WSE is below a threshold for a predefined period of time.

Both base and alternative WSE enabling (*WSE On/Off*) subcontrollers contain a status hold in each of the states for a prescribed time period.

There is a significant difference between the two design cases when it comes to the CW-loop control: namely, the alternative design makes use of the *CW reset*, as illustrated in the control chart on the top right in Figure 2. The main differences can be summarized as:

- The base design CW-loop pumps and cooling tower fans are operated at constant full speed. A three-way mixing valve maintains minimum chiller lift as it helps elevate the CW supply temperature at times when the cooling tower capacity is high due to cold weather. The modulation is performed using a PI controller to maintain the actual PLR_{ch} above its minimum $PLR_{ch,min}$.
- In the alternative case the ASHRAE G36-based head pressure and tower fan subcontrollers provide tower and/or pump speed modulation.

Figure 2 illustrates the CW reset control diagram. The tower fan speed set-point $r_{t,set}$ is modulated between its minimum and maximum limits, using PI controllers that are specific for the operating mode: WSE-only, integrated, chiller-only.

In the WSE-only mode, the control objective of the tower fan speed set-point $r_{t,set}$ is to keep the $T_{chw,s}$ at its set-point. If the WSE is enabled, the maximum tower speed set-point is set to its maximum value $r_{t,set,max}$, the CW pump is commanded to operate at full speed $r_{cwp,set} = 1$, and the chiller isolation valve modulates down linearly with the control signal $u_{l,ch}$ to reduce the flow through the chiller to maintain the minimum lift. When the WSE is disabled, the CW reset

logic keeps the modulation valve $y_{ch,c,m}$ fully open, while the cooling capacity reduction is achieved through a reduction in the maximum allowable tower fan speed $r_{t,set,max}$. Should this not suffice, the pump flow rate would be reduced through modulating the speed of the chilled water pump $r_{cwp,set}$.

In real applications there exist simpler versions of the condenser water reset—for instance, a few discrete fan speeds to assure safe chiller operation at low chiller lift. For contrasting purposes, we chose to compare full speed in the base case with the variable speed modulation in the alternative case.

The next section elaborates on the selection of physical sizes and other parameters needed to complete the design and do the software implementation.

Sizing and parameterization

In this section, we present the set of assumptions driving the plant component sizing and controls parameterization decisions, both on the demand and on the supply side. As the article primarily aims to demonstrate the process, the tools, and the techniques to evaluate control sequences and system configurations, we defined a reasonable set of sizing parameters in terms of thermal loading, component nominal capacities, and hydronic configurations.

We defined the sizing and parameterization assumptions based on literature research and expert knowledge. We configured the controllers with an intent to allow for a fair comparison between the cases.

Data center

For simplicity, we assume the data center room is adiabatic and there is no humidity control. Furthermore, for overall system sizing and evaluation purposes, we assume that data center is constantly running at about 30% of the full capacity, the same as in the example in Rasmussen (2007). As a further reference, the average utilization rate for service provider servers reported in Shehabi et al. (2016) is 25%.

On the demand side we take as a design assumption a data center with a total thermal output of 500 kW, including sources outlined in Rasmussen (2007), such as information technology (IT) loads, uninterruptible power supplies (UPSs), lighting, power distribution, and personnel. We assume that non-IT equipment other than the cooling system makes up on average 20% of the data center zone load. We were not aiming to represent a particular type or generation of data centers; rather, we were looking for a reasonable value to evaluate the benefits of energy savings achieved through alternative cooling controls. We reduced the value of 29% identified in the cited source to 20%, as the nominal capacity of the data center from the source is twice smaller than our assumed data center thermal load. Based on Shehabi et al. (2016), a larger data center is generally more efficient due to economies of scale.

The cooling system waste heat is not considered to be a part of the thermal load, as the location of the cooling system is assumed sufficiently outside of the data center zone.

The non-IT loads including the total cooling energy make up about 24% of the total facility energy.

The layout of the data center equipment is assumed to follow ASHRAE best practices recommended in ASHRAE (2015) and is, therefore, using a data center zone supply air temperature set-point of 27°C for the “cold aisle.” The air distribution is assumed directly into a cold aisle plenum, after a short duct.

Chiller plant

The cooling system is sized to reliably meet the data center’s cooling load at the given location. Based on the current thermal tolerance of the IT equipment, we select a server room air temperature set-point (cold aisle) $T_{z,s, set}$ of 27°C in the main analysis, as originally set for the plant in Wetter et al. (2014) and also mentioned in ASHRAE (2015).

We selected a fixed speed chiller available in MBL, with a nominal capacity of 471 kW. The effective cooling capacity of the chiller depends on the outdoor air and loading conditions. The effective capacity of the selected chiller suffices due to the high zone supply air temperature set-point $T_{z,s, set}$ and the selected climate’s wet-bulb outdoor air temperature $T_{oa,w}$. The conditions allow a plant with a generously sized WSE and a chiller sized tightly to the load to achieve a near $N + 1$ cooling capacity redundancy.

The nominal air and water mass flow assumptions are:

- The air flow rate in the supply air loop is 33 kg/s. It is calculated assuming a temperature difference across the coil of 15 K. With these parameters the supply air fan achieves an airflow efficiency ratio (AER) of 0.11 W/(m³/h), similar to the first example provided in Petschke (2021).
- The water flow rate in the CHW loop is 12 kg/s. This is selected as both a value with a design temperature difference of 10 K and one close to the selected chiller model design condition. The chosen value also fits the rule from Trane (2014).
- The water flow rate in the CW loop is 20 kg/s for each chiller condenser and WSE. The value is near the chiller model design condition and falls within the standard industry range (AHRI 2020).

Nominal pressure drops through heat exchangers, pipes, and fittings were assumed to be as follows:

- The chiller evaporator has a pressure drop of 19 kPa, while for the chiller condenser we assumed 42 kPa. To calculate the values we developed a scaling approach to a chiller specification of Carrier Corporation (2014), and corrected the values to fit our chiller’s nominal cooling capacity, CW, and CHW flows. We assume that the tubes of the shell-and-tube heat exchanger for a comparably slightly smaller chiller, such as the one we applied in the model, would be a bit narrower such that at a cooling capacity proportionally adjusted nominal flow they would cause the same pressure drop as specified in the source. Then we scaled the nominal pressure drops from the data with the square of the ratio of the model nominal flows and the adjusted flows. The square relationship stems from the Bernoulli equation.

- The cooling tower pressure drop is primarily due to overcoming the height difference based on BAC (2013). Assuming a 1.5 m tall cooling tower, its pressure drop is estimated at 15 kPa.
- Regarding the cooling coil, assuming discrepancies in airflow and water flow are accounted for through placing coils similar to those provided in Trane (2019) in parallel to each other, we adopted pressure drop values close to values found in the source. On the air side we assume the coil as the main flow-resisting element, while any short ducts and plenum add about 5–10% to obtain a total air-side pressure drop of 200 Pa. On the CHW side we assume a pressure drop of 24 kPa.
- For the WSE we assume the same CW flow and thus the same pressure drop as for the chiller condenser, 42 kPa, as suggested in Taylor (2014). We then scale the CW WSE pressure drop according to the CHW-side flow, to obtain the CHW-loop WSE pressure drop of 15 kPa.
- We assume pipe diameters of 6 inches (~15 cm) for CW, and 5 inches (~13 cm) for CHW loop. The CHW contains 30 m of piping for both base and alternative case. The alternative controller is assumed to also have 30 m of pipes in the CW loop, while the base controller has 10 m of pipes in each chiller condenser and WSE CW-side loops, with another 20 m of piping in the cooling tower loop. The piping pressure drops were selected based on pressure drop tables from Advantage Engineering (2021) and doubled to encompass both piping and simple fittings excluding modulated valves. The resulting values are: 4.5 kPa in the CHW loop, and in the CW loop, 4.3 kPa in the alternative and 5.7 kPa in the base case; 6 kPa is added to account for any modulating control valves (Belimo Aircontrols 2021).

The cooling tower approach is assumed at 4 K, which is slightly more conservative than in the examples from PG&E (2012). Based on a sizing rule from AHRI (2020) that relates the tower fan power to the chilling capacity, the tower fan is sized at 6.5 kW.

Lastly, here we list some of the main controller parameters set in both cases to ensure comparability:

- Chilled-water supply temperature set-point $T_{chw,s, set}$ is limited between 5.56 and 22°C.
- Chilled-water differential pressure set-point $dp_{chw, set}$ ranges from 12,970 to 129,700 Pa.
- Temperature dead-band for the chiller enable hysteresis switch equals 2.2 K.

The modeled configurations use typical values for the minimum pump speeds and modulation valve positions, among other technical requirements. For actual installations, these would be determined and set at commissioning to assure the minimum flow through the chiller evaporator and condenser, and to meet the minimum lift.

The parameters presented in this section are summarized in Table B1 in Appendix B. The list of parameters is not exhaustive, as many parameters are set as default or calculated directly in the models. All controller parameters can be

further explored in the open source models following the first link provided in the “Conclusion” section.

Software implementation

We implemented all models using the Modelica⁴ modeling language. The models, detailed sizing rules and assumptions, and simulation result visualization capabilities are freely available on the OBC project Github repository. The alternative controller is implemented in CDL. We utilized the Python⁵ programming language to perform simulation data analysis and to visualize the results. The “Conclusion” section provides links to the software implementations and the libraries.

In the simulation models, idealizations were made regarding the devices’ proven on status. That is, when the device is commanded on or off, we assume that the device’s proven on or off status instantaneously equals it. Similarly, a differential pressure or speed set-point sent to a pump or a fan are assumed to be reached instantaneously, so that the control logic assumes, for instance, $dp_{chw,set} = dp_{chw}$.

The following subsections describe the closed-loop chilled water plant, elaborate on controls system model development, and present the control logic implementations.

Chilled water plant coupled with deterministic controls

The case study models, including the base case subcontrollers, and the ASHRAE G36-based chiller plant control models are composed into Modelica packages. Structurally, the closed-loop system model implementations resemble the design plant and control diagrams from Figures 1 and 2. Each model consists of:

- A TMY3 weather data reader representing the local environment.
- Model blocks that map to the control sections in Figure 1 for the base case and Figure 2 for the alternative case control design.
- A chiller plant model including the CHW loop exchanging heat with the air loop through the cooling coil, with the CW loop through chiller or WSE, or both, and a CW loop connected to the environment through the cooling tower model.
- The data center cooling zone model placed in the air loop, linked to the CHW loop by a cooling coil.

The hydronic and air loops are formed using connectors between the appropriate ports provided in all equipment model class instances (e.g., $T_{chw,r}$ measuring thermostat model is connected to the base design’s chiller on/off status controller model and to the chiller/WSE staging controller model in the alternative design case). Appendix A provides the graphical model illustrations of the implemented closed-loop system models.

High-performing control sequences: Implementation from software libraries

The controllers were modularized into device-level subcontrollers, such as the cooling tower, the chiller staging, and the water-side economizer controller.

In both design cases, we instantiated each of the device controllers, further referred to as subcontrollers, parameterized them, and connected them to sensors and actuators. The subcontrollers follow a simple hierarchical structure, as illustrated in Figure 3 for the chiller/WSE staging controller instantiation example, starting from the top level to sequence layers, subsequence layers, and to elementary blocks.

The alternative controls use the CDL language, which will in the future be in compliance with the proposed ASHRAE Standard 231 P. The base case controller utilizes blocks from both the MSL and the MBL.

The end-use modeler, as opposed to the control sequence developer, does not need to know about the controller structure. The modeler is primarily exposed to the parameterization panels of each controller. Figure 4 shows the example parameterization panels and the input/output interfaces of the chiller staging controller used in the alternative case.

Experimentation environment

To evaluate the system performance over the time period of one year and one summer season for both configurations, we conducted a number of simulation experiments with the Dymola 2021 environment.⁶ We performed both main and sensitivity analysis simulations using the Dassl solver with a tolerance of 10^5 .

Results

In the following subsections we present:

- Overall and device-level power usage effectiveness (PUE) and energy use for the annual and summer season. We provided results for the main analysis scenario with the zone supply air temperature set-point $T_{z,s,set}$ of 27°C, as well as for the sensitivity analyses with the $T_{z,s,set}$ set to 25°C, to better understand the impacts of lower zone supply air temperature set-point, and to 29°C, to evaluate the impacts of higher zone supply air temperature set-point.
- A simulation-based engineering approach to determine the designs’ viability of chiller-free operation in any climate.

Comparative performance

Figure 5 shows annual and summer season energy use and PUE for both design cases.

The alternative case is 25% more efficient annually, and 18% more efficient during summer. Because of the CW reset, the tower fan energy use of the alternative design case is annually about 88% lower than for the base case, and 67% lower in the summer. The CW reset reduces the

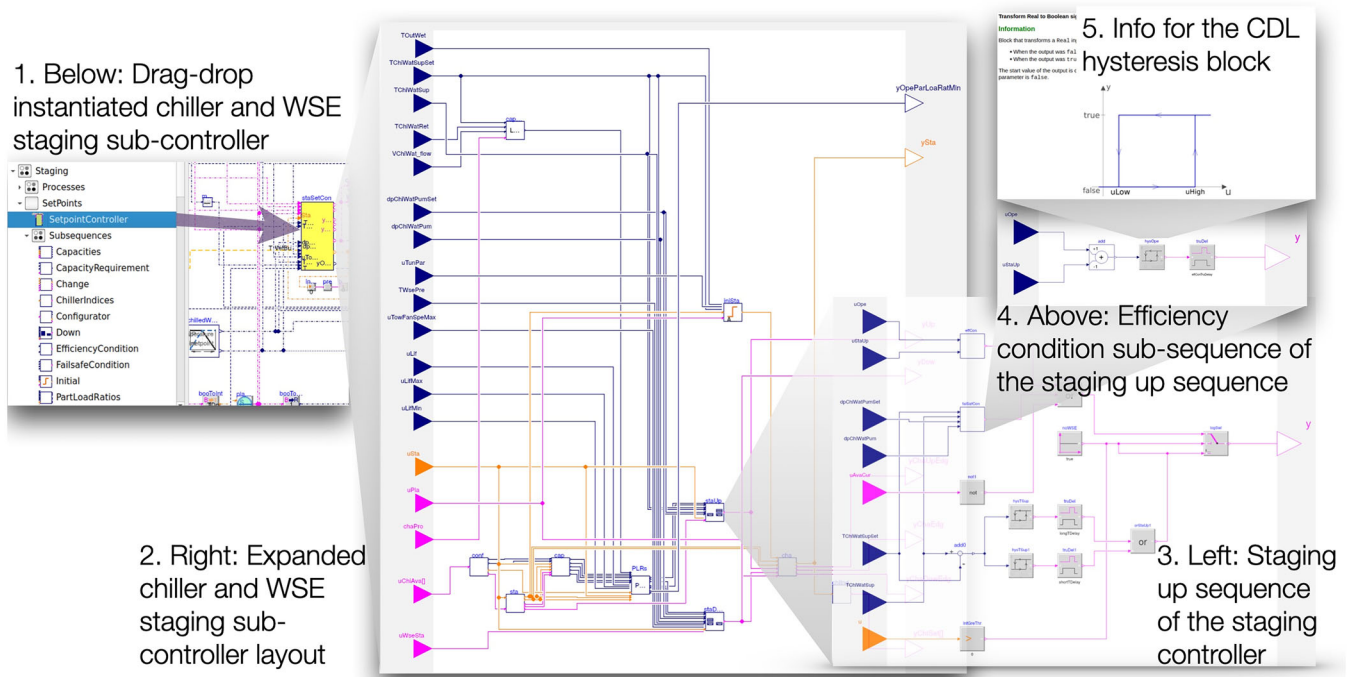


Fig. 3. Controller model instantiation from the MBL control sequences package (1) and a walk through (2, 3, 4) the controller model hierarchy for the example of the chiller staging controller. The staging controller consists of several control sequences, where each may have additional underlying layers. Each model layer contains model information, here illustrated on the elementary CDL block level (5).

staSetCon in ChillerPlant.ClosedLoopAlternative.OneDeviceWithWSE

General Time parameters Conditionals Add modifiers Attributes

Component

Name: staSetCon

Comment: Single chiller with WSE staging controller

Model

Path: Buildings.Controls.OBC.ASHRAE.PrimarySystem.ChillerPlant.Staging.SetPoints.SetpointController

Comment: Calculates the chiller stage status setpoint signal

Plant configuration parameters

have_WSE: true (true = plant has a WSE, false = plant does not have WSE)

have_serChi: false (true = series chillers plant, false = parallel chillers plant)

anyVsdCen: false (Plant contains at least one variable speed centrifugal chiller)

Chiller configuration parameters

nChi: 1 (Number of chillers)

chiDesCap: {471000} (Design chiller capacities vector)

chiMinCap: {0.1*471000} (Chiller minimum cycling loads vector)

chiTyp: StageTypes.constantSpeedCentrifugal (Chiller type. Recommended staging order: positive displacement, variable speed centrifugal, constant speed centrifugal)

nSta: 1 (Number of chiller stages)

staMat: {{1}} (Staging matrix with stage as row index and chiller as column index)

Hold and delay parameters

avePer: 300 (Time period for the capacity requirement rolling average)

delayStaCha: 0.25 (Hold period for each stage change)

parLoaRatDelay: 0.25 (Enable delay for operating and staging part load ratio condition)

faiSaTruDelay: 0.25 (Enable delay for failsafe condition)

effConTruDelay: 0.25 (Enable delay for efficiency condition)

shortTDelay: 0.166666666666667 (Short enable delay for staging from zero to first available stage up)

longTDelay: 0.333333333333333 (Long enable delay for staging from zero to first available stage up)

Staging part load ratio parameters

posDisMult: 0.19 (Positive displacement chiller type staging multiplier)

conSpeCenMult: 0.0 (Constant speed centrifugal chiller type staging multiplier)

anyOutOfScomult: 0.0 (Outside of G36 recommended staging order chiller type SPLR multiplier)

varSpeStaMin: 0.45 (Minimum stage up or down part load ratio for variable speed centrifugal stage types)

varSpeStaMax: 0.0 (Maximum stage up or down part load ratio for variable speed centrifugal stage types)

Value comparison parameters

smallITDif: -270.95 (Offset between the chilled water supply temperature and its setpoint for the long condition)

largeITDif: -270.95 (Offset between the chilled water supply temperature and its setpoint for the short condition)

faiSaITDif: -272.15 (Offset between the chilled water supply temperature and its setpoint for the failsafe condition)

dpDif: 2*6895 (Offset between the chilled water pump differential static pressure and its setpoint)

TDif: -271.15 (Offset between the chilled water supply temperature and its setpoint for staging down to WSE only)

TDifHys: -272.15 (Hysteresis deadband for temperature)

faiSaDpDif: 2*6895 (Offset between the chilled water differential pressure and its setpoint)

dpDifHys: 0.5*6895 (Pressure difference hysteresis deadband)

effConSigDif: 0.05 (Signal hysteresis deadband)

Fig. 4. Input-output structure and parameterization panes of the chiller and WSE staging controller.

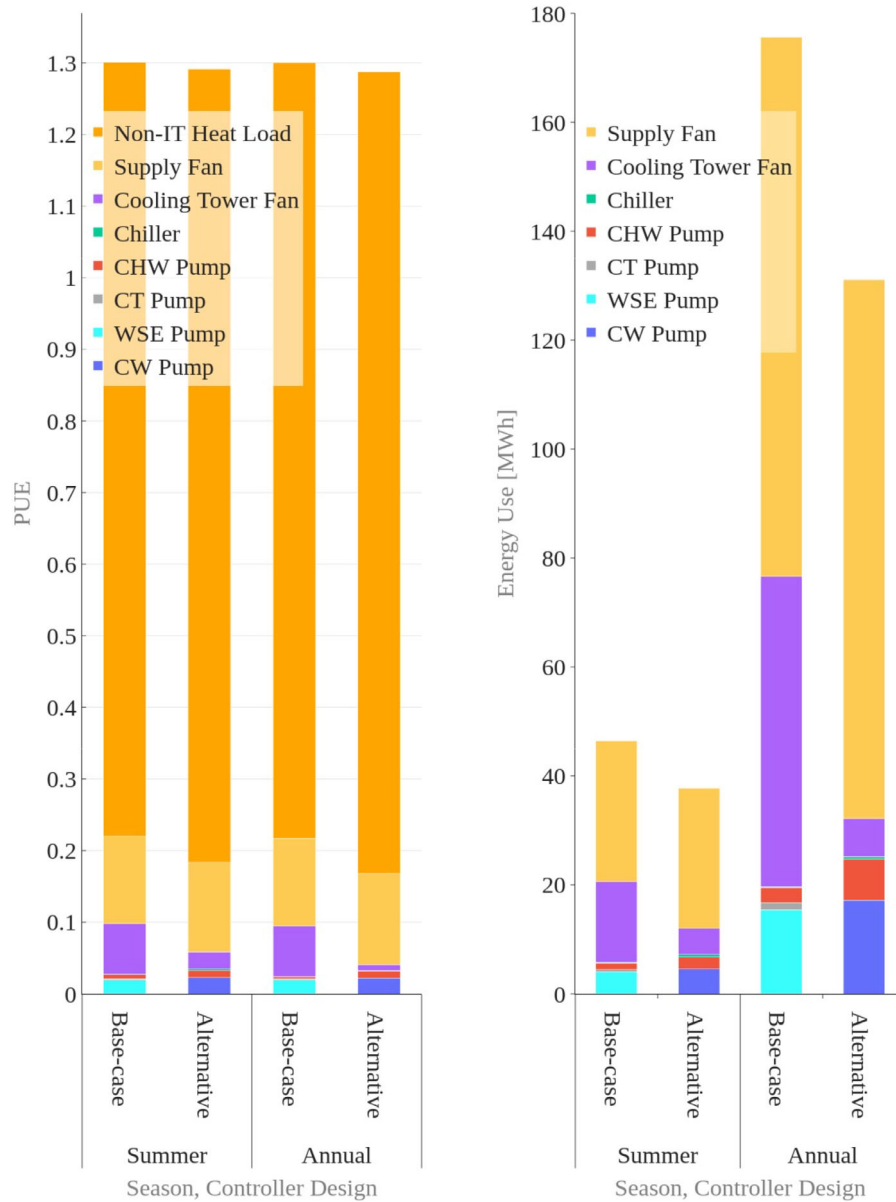


Fig. 5. Comparative power usage effectiveness (PUE), left, and energy use, right, annual and summer bar charts with a device-level disaggregation. Note: CW pump legend entry represents the only CW-loop pump in the alternative and a dedicated chiller CW-loop pump in the base case.

average annual tower fan speed r_t in the alternative case by 71%. This causes a rather significant, but less consequential, increase in CHW pump power consumption: 157% in the summer and 62% during the winter when compared to the base design case. The CHW pump consumes less in the base case, as the cooling tower always provides the maximum capacity to the WSE. The reduction in tower fan speed in the alternative case increases the WSE cooling water temperature, thereby requiring a higher reset on the CHW side that elevates the $dp_{chw,s, set}$ compared to the base case, with the annual averages at 38kPa in the alternative and 18kPa in the base design case. The supply air fan power consumption is identical across the design cases.

The reduction in average tower fan speed r_t is large because in the base case the tower fan speed r_t is constant. If we were to compare the full modulation, as implemented in the alternative case, with some simpler fan speed modulation common in the field (e.g., two fan speeds), the resulting energy savings would be lower.

Integrated operating mode occurs when both the chiller and the WSE are enabled. The plants operate in the integrated mode for only 0.3% of the year in the alternative, and for 0.1% of the year in the base design case. As the WSE is enabled all the time, the chiller energy use is negligible, and more so in the base design case. The CW-side pump energy in the base case is, effectively, representing only the energy

use of the CT and the WSE pumps, while the dedicated chiller condenser pump energy use is too small to be visible on the graph. The total CW-loop pump energy use in the base design case, consisting of the CT and WSE pump energy use, approximately equals the energy use of a single CW pump in the alternative design case. As the WSE is enabled all year, the CW pump speed also remains constant in the alternative case, allowing for such direct comparison.

A large fraction of the annual PUE is attributed to non-IT loads (primarily power systems such as UPSs, transformers, and PDUs) other than cooling. The small differences between the cases' PUE values are caused by the reduction in tower fan power consumption in the alternative case.

In the next subsections we describe the data center load sensitivity analyses and illuminate how a small excerpt of a control sequence had a significant effect on the plant performance and design under varying weather conditions.

Sensitivity to zone supply air temperature set-point

We performed sensitivity analyses to determine the impact of a change in the data center zone supply air temperature set-point $T_{z,s,set}$ of 2 K. In each sensitivity analysis we maintained a 5°C difference between the maximum chilled water

supply temperature set-point $T_{chw,s,set,max}$, and the zone supply air temperature set-point $T_{z,s,set}$, to prevent low chiller lift at startup.

Figure 6 provides the PUE and the energy use comparison among design cases and seasons, for the two sensitivity analyses. When the zone supply air temperature set-point $T_{z,s,set}$ increases, the alternative controller incurs savings of 28% annually, and 26% in the summer. With the $T_{z,s,set}$ decrease of 2°C, the alternative controller saves 11% of the energy used annually, but causes the base controller to outperform the alternative design by 23% during the summer season. This phenomenon is mainly due to the control logic difference in switching from the integrated into WSE-only mode. The reason is as follows.

With the elevated zone supply air temperature set-point $T_{z,s,set}$ at 29°C, the chiller becomes fully redundant in both the base and the alternative case in the given climate. Not surprisingly, the decrease to 25°C results in some time spent in the integrated economizer operation mode, 5% of the year in the base and 15% in the alternative case.

The device-specific bar plots on the right side of the Figure 6 show that for annual operation, the main increase

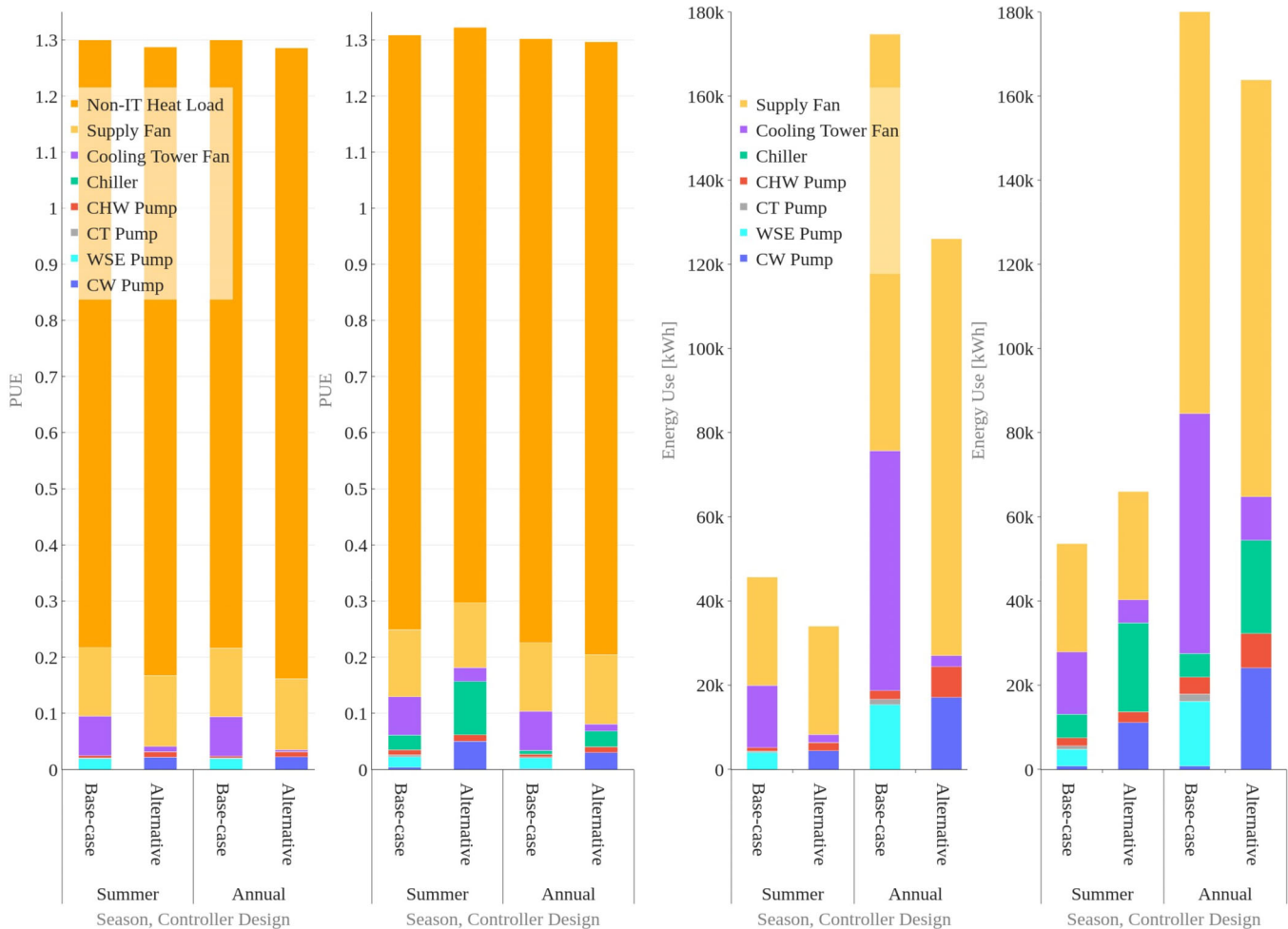


Fig. 6. Sensitivity to data center air supply temperature set-point. Left to right: Power usage effectiveness (PUE) at 29°C and 25°C, and energy use at 29°C and 25°C. Legend reflects categories illustrated from top to bottom.

in energy use caused by the decrease in $T_{z,s,set}$ stems from the chiller, compared to the simulation with the increased set-point, where the chiller does not get enabled at all. Higher chiller energy use is showing across the control cases and seasons, and it is most pronounced for the summer season in the alternative design case. As the CT fan speed modulates in the alternative case, the CT energy use also significantly increases with the lowering of the $T_{z,s,set}$.

The change in PUE is barely noticeable with the increase in $T_{z,s,set}$, while its decrease causes slightly higher summer season and equal annual PUE for the alternative and base case designs.

Appendix C provides numerical values for energy use in Table C1 and PUE in Table C2 for the three air supply temperature set-points: the main analysis and the two sensitivities.

Impact of staging into WSE-only operating mode logic

What appear to be small differences in the control logic may have significant effects on the control performance. This section serves to provide such an example.

The operating modes during annual simulation in Sacramento for the given system are predominantly WSE-only, with a negligible fraction of time spent in integrated economizer operation. Consequently, we know that the WSE operates during the entire year. To better understand the conditions that led to integrated economizer operation instances for each of the design cases, we show the plots on Figure 7.

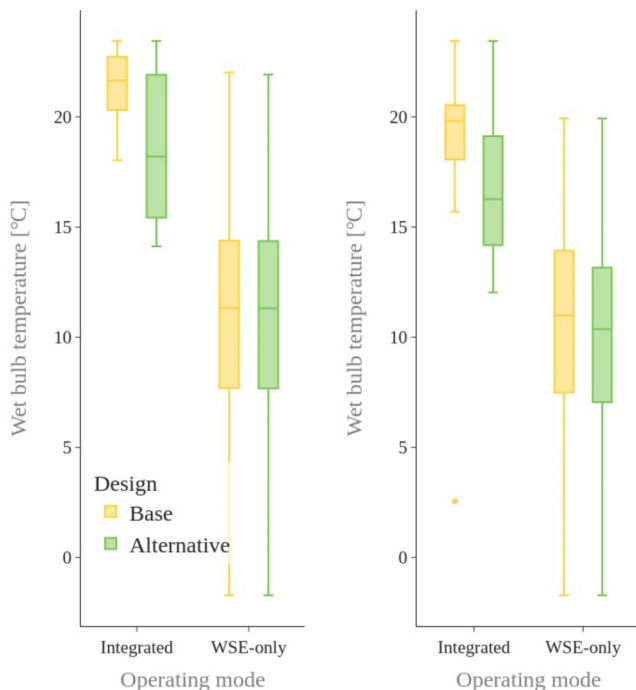


Fig. 7. Distributions of air wet-bulb temperatures $T_{0a,w}$ occurring during a year of simulated performance for each operating mode and design case. Main analysis is illustrated on the left with the zone supply air temperature set-point $T_{z,s,set}$ at 27°C, and the sensitivity analysis with $T_{z,s,set}$ reduced to 25°C is on the right. The boxes represent the interquartile range (between the 25th and the 75th percentile) and the whiskers are at the 5th and the 95th percentile.

The comparative box plots display the distribution of wet-bulb temperatures $T_{0a,w}$ that occur during the annual operation, for the main zone supply air temperature set-point $T_{z,s,set}$ of 27°C and the sensitivity that assumes the set-point is reduced to 25°C. Comparing the two set-point analyses, the integrated economizer operation for the lower zone supply air temperature set-point $T_{z,s,set}$ showed a lower range of wet-bulb temperatures $T_{0a,w}$ compared to the 25°C set-point, as expected. This occurred as the WSE-only operating mode can be used at higher wet-bulb temperatures $T_{0a,w}$ if the zone set-point $T_{z,s,set}$ is higher.

Looking at the plots, we also observe an interesting difference between the two design cases, present in both the main analysis and the decreased zone supply air temperature set-point $T_{z,s,set}$ sensitivity. While the range of outdoor air wet-bulb temperatures $T_{0a,w}$ in the WSE-only operating mode was similar to identical among the sensitivities and design cases, in the integrated operation mode the chiller remained enabled at significantly lower outdoor wet-bulb temperatures $T_{0a,w}$ for the alternative compared to the base design case. This difference, further illuminated in the next couple of paragraphs, is caused by a small control logic difference in staging down conditions when stepping into the WSE-only operating mode.

In Figure 8 we illustrated a detail of the control performance that drives the observed difference in outdoor air wet-bulb temperatures during which the chiller remains enabled. The figure shows 5 hours of summer plant operation of the integrated economizer operating mode. The chiller enable/disable status lasts for more than an hour longer in the alternative design case, as the staging controller logic is utilizing a condition to enable the chiller that is different from the condition to step back into WSE-only mode.

The upper plot shows the base case control behavior, where the chiller is switched on when the temperature difference between the CHW temperature downstream of the WSE $T_{chw,r,d}$ and the CHW supply set-point temperature $T_{chw,s,set}$ crosses the hysteresis deadband. Once the temperature difference gets back to zero, the chiller is disabled.

In the alternative case, shown in the bottom plot, a similar chiller enable condition was activated at a similar moment as for the base controller. Once the difference between the chilled water supply $T_{chw,s}$ and its set-point $T_{chw,s,set}$ reached the deadband, the chiller was enabled. The chiller, however, remained enabled until the downstream of the WSE temperature prediction $T_{chw,r,d}$ was sufficiently below the CHW supply set-point $T_{chw,s,set}$. Over the course of the year, this difference in staging down condition is significant to drive higher alternative design case summer energy use for the low zone set-point sensitivity, as we discussed in the previous subsection and showed in Figure 6. In real applications such an approach to chiller disable logic may prove to be more reliable, for example, in reducing chiller enable instances, even though it causes somewhat longer cumulative chiller enable time.

For further reference we named the type of the chiller enable/disable status hysteresis, as implemented and explained for the alternative design case, asymmetrical.

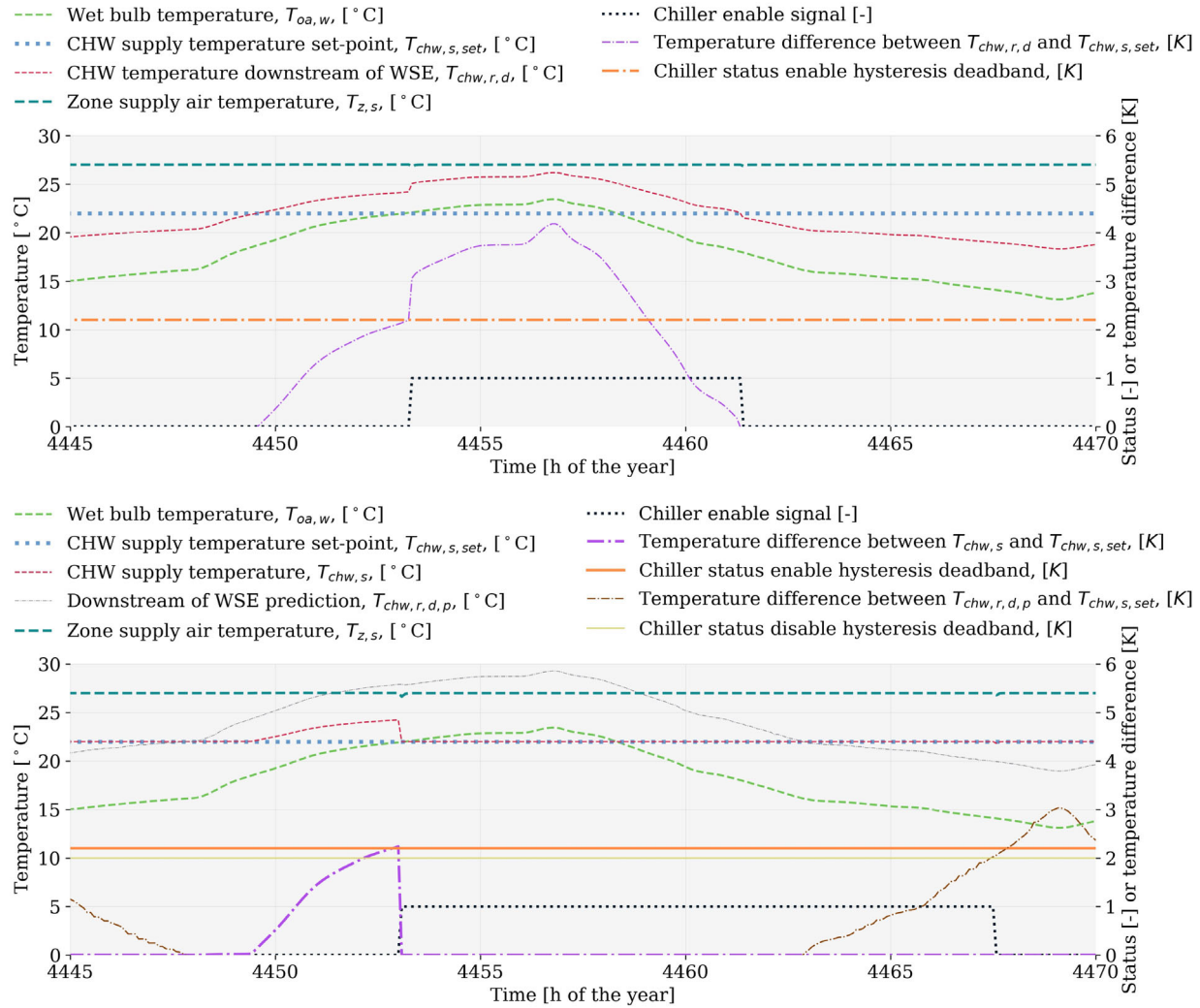


Fig. 8. Comparative time-series plots of the chiller enable/disable behavior. Top: base case. Bottom: alternative case.

Example application as configuration and sizing design aid

In the preceding, we saw that the asymmetrical hysteresis effect caused prolonged chiller enable time and increased the energy use when the zone supply air temperature set-point $T_{z,s,set}$ was decreased. This claim is also illustrated through the large range overlap between the integrated economizer operation and that of the upper quartile of the WSE-only operation we saw in Figure 7.

This raises a question on how high a wet-bulb temperature $T_{oa,w}$ for how long causes the chiller to switch on. The knowledge would help determine whether a chilled water plant can operate without a chiller, and it allows one to predict the operating modes in any climate. Knowing the operating mode timing, duration, and frequency can be used for planning purposes, for example, for plant maintenance, redundancy, power purchasing, risk mitigation, and so on.

The plant is parameterized such that the highest CHW supply temperature set-point $T_{chw,s,set,max}$ is 22°C. Consequently, we know that the outdoor air wet-bulb temperature $T_{oa,w}$ continuously at or above 22°C would eventually cause the chiller to switch on. How quickly and at

which wet-bulb temperature value depend on the system dynamic and parameters, for example, the value of $T_{z,s,set}$ and thermal inertia of the system.

Here we introduce and apply a system-specific and climate-agnostic simulation-based design method that does not require explicit knowledge about the plant and control models to determine the second law of thermodynamics $T_{oa,w}$ governed limit for WSE-only operating mode, valid in any climate for a given sized and parameterized system. For such simulations we use the outdoor air wet-bulb temperature $T_{oa,w}$ ramp signal, slow compared to the given system thermal inertia with delays introduced by controls, as illustrated by green lines in Figure 9. In the upper row the plots provide the results where the black dotted line representing the chiller enable signal crosses the green line indicating the wet-bulb temperature $T_{oa,w}$ ramp. The $T_{oa,w}$ limit is read off where the chiller enable signal crosses the temperature ramp, yielding almost 22°C in both cases, reflecting the $T_{chw,s,set,max}$ of 22°C, well designed controls, and efficient heat exchangers. This means that for any climate where the wet-bulb temperature does not ever exceed 22°C, the chiller-free plant design can be considered. For the sensitivity

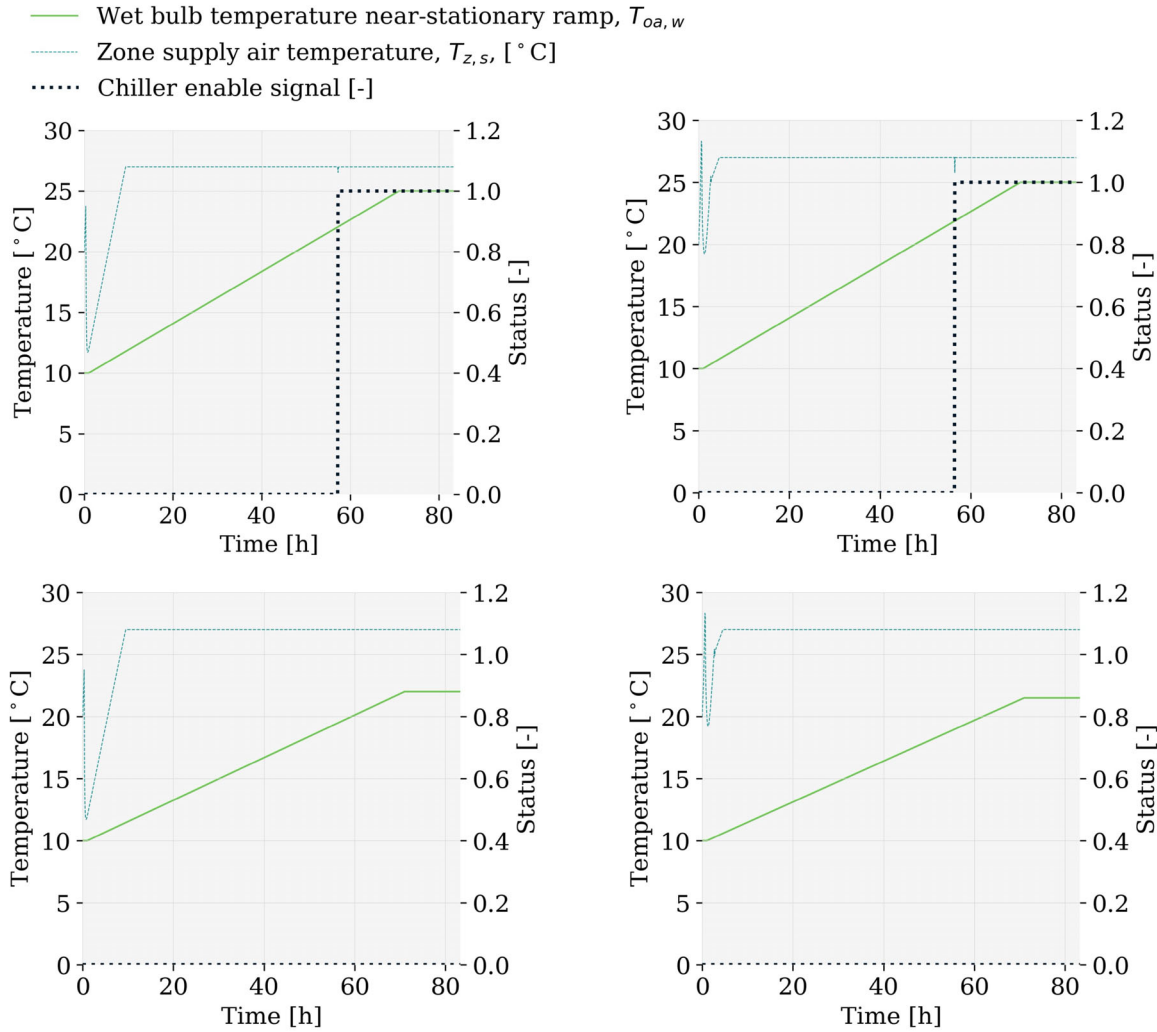


Fig. 9. Determining design-specific WSE-only operating mode wet-bulb temperature limit. Upper row: Simulation to determine the minimum chiller enable $T_{oa,w}$ limit for base case (left) and alternative case (right). Lower row: Verification of maximum $T_{oa,w}$ limit that ensures WSE-only operating mode. Zone supply air temperature set-point is 27°C.

analysis with the zone supply air temperature set-point $T_{z,s,set}$ at 25°C and the $T_{chw,s,set,max}$ at 20°C, the limit is at nearly 20°C, as anticipated.

Using the same simulation setup, we can identify a slightly lower temperature that we may declare, upon verification by simulation, the upper $T_{oa,w}$ limit for sufficiently long duration of the WSE-only operating mode, as shown in the lower row of the subplots in Figure 9. A duration of 10h suffices for the analysis, as this is long enough to represent the duration of continuous peak heat on a summer day, and as this is much faster than the system dynamics. The testing is performed with the upper ramp limit placed at the estimated $T_{oa,w}$ limit for WSE-only operation; in the plots, that is 22°C for the base and 21.5°C for the alternative case.

The presented nearly stationary wet-bulb temperature ramp method is useful as it allows for systematic determination of the highest wet-bulb temperature under which the cooling system would still operate using the WSE only and

without a chiller. Ideally, one would automate the redesign iterations until the climate-specific wet-bulb temperature WSE-only test would pass. As the temperature data are known, once performed the test for a given load would always apply. Given a list of design wet-bulb temperatures per location and a set of interesting loads, one could use simulation to create engineering recommendation databases for chiller-less cooling plant design.

Conclusion

We presented and illustrated the model-based comparative co-design process that allows performance of design evaluation of the simulation performance of two data center chilled water plants and control sequences.

Due to the complexity of the high-performing control algorithms, simulation is well suited to compare their

performance. Having access to open source control sequence libraries significantly reduces the effort involved in setting up such simulation models. Engineering design of data center cooling systems involves making a large number of decisions. The number of viable designs is a consequence of the interplay between the hydronic configuration, controls, climate, component sizing from selecting WSE and chiller capacity to sizing the pipes, and estimated future use of the data center. Evaluation of options can easily turn into a costly exercise. We showed that even small differences in the control logic can have significant impact on plant performance. The impact of such differences may heavily depend on the climate conditions, strengthening the case for annual simulation base performance comparison. Furthermore, the design of control sequences themselves may benefit from the ability to perform simulation-based testing and performance comparison.

We also touched upon the possibility of chiller-free design solutions. For the future we may envision distributed data center resources that rely heavily on chiller-free operation. Traditionally, the chiller plant resilience was linked to locally available redundancy. In the era of cloud computing, it may be possible for the users to switch to a currently chiller-free operating data center, depending on the match between the computation demand and weather conditions. Such distributed redundancy may allow for a lower on-site redundancy requirement.

If such a distributed network of data centers were built robustly and tied with weather and power generation predictions, the first cost associated with the chiller and any related equipment (e.g., pumps, fittings) could be reduced. The data center network would ideally be in varied time and climate zones, to offset effects of extreme weather occurrences at any one location. Higher and more expensive data center redundancy levels would remain reserved for those rare services that truly need to be up all the time. Notably, there may be an increase in cooling tower water use for the chiller-free systems—a trade-off worth additional resource adequacy analysis.

The work showed three dimensions of model-based design: We used a controls design process that leverages high-performing standardized control sequences, we demonstrated it by analyzing the performance of data center chilled water plant designs, and we identified further engineering, planning, and design applications of the simulation models.

Software availability

The case-study models and analytical capabilities are available on the OBC project Github repository.⁷ The models rely on MSL 3.2.3⁸ and the MBL.⁹ The alternative controller packages are available on the MBL Github repository.¹⁰ The CDL package¹¹ is implemented in MBL. The postprocessing algorithms and visualizations utilizing open source Python libraries are available in a Jupyter Notebook.^{12,13}

We use the following nomenclature:

Nomenclature

- CHW, CW, = chilled water, condenser water, and
and CT = cooling tower.
DP = differential pressure.
IT = information technology.
MBL, MSL = Modelica Buildings Library and Modelica
Standard Library.
PI = proportional-integral feedback controller.
PLR = part load ratio.
PUE = power usage effectiveness.
TMY = typical meteorological year.
T&R = trim and respond feedback controller.
WSE = water-side economizer.
 ch, c, wse, p = device subscripts, respectively: chiller,
condenser, WSE, any pump (CHW pump,
CW pump, WSE cooling pump, and CT
pump).
 s_x = on/off status for device x .
 \dot{V}_x = volume flow rate for device x .
 $X_{y, set}$ = set-point for variable X_y .
 $X_{y, min}$ = minimum limit for variable X_y .
 $T_{oa}, T_{oa, w}$ = outdoor air dry and wet-bulb temperature,
and $T_{oa, l}$ = and lower outdoor air temperature limit
for plant enable.
 $T_{cw, r}$ and $T_{cw, s}$ = CW return and supply temperatures
supply flows from the CT to the
condenser.
 $T_{chw, s}, T_{chw, r}$ = CHW supply, CW return, CW return
 $T_{chw, r, d}$ = downstream of WSE temperature, and its
and $T_{chw, r, d, p}$ = predicted value.
 dp_{chw} = CHW loop DP.
 $T_{z, s}$ = zone supply air temperature.
 r_t and r_{cwp} = CT fan speed and CW pump fan speed.
 PLR_{ch} = chiller operating PLR.
 $u_{chw, pr}$ = CHW plant reset control signal (maintains
 $T_{z, s}$ at set-point).
 $u_{l, ch}$ = head pressure control loop signal that
aims to maintain the difference between
the $T_{chw, s}$ and $T_{cw, r}$ above a design
minimum chiller lift.
 $y_{ch, c, m}$ = CW flow modulating valve position.
 r_t = CT fan speed.
 r_{cwp} = CW pump speed.
 PLR_{wse} = WSE heat exchanger flow rate PLR with
respect to nominal.
 $dT_{t, app}$ = CT approach (minimum resulting heat
exchange temperature difference).
 $dT_{wse}, dT_{wse, on},$ = temperature differences used in enabling
 $dT_{wse, off},$ and disabling chiller and WSE.
and $dT_{ch, on}$

Units and additional abbreviations are provided directly in the text where needed.

NOTES

1. <https://obc.lbl.gov>
2. <https://www.ashrae.org/technical-resources/standards-and-guidelines/titles-purposes-and-scopes>
3. <https://taylorengeers.com>
4. <https://modelica.org>
5. <https://www.python.org>
6. <https://www.3ds.com/products-services/catia/products/dymola>
7. <https://github.com/lbl-srg/obc/commit/6458d9a621>
8. <https://github.com/modelica/ModelicaStandardLibrary/tree/maint/3.2.3>
9. <https://simulationresearch.lbl.gov/modelica>
10. <https://github.com/lbl-srg/modelica-buildings/commit/5f32171b19>
11. <https://github.com/lbl-srg/modelica-buildings/tree/master/Buildings/Controls/OBC/CDL>
12. https://github.com/lbl-srg/obc/blob/issue40_caseStudy_dataCenter/examples/case_study_2/post_process.ipynb,commit2af6c56
13. <https://jupyter.org>

Acknowledgments

This research was supported by the Assistant Secretary for Energy Efficiency and Renewable Energy, Office of Building Technologies of the U.S. Department of Energy, under contract no. DE-AC02-05CH11231, and the California Energy Commission's Electric Program Investment Charge (EPIC) Program.

Disclosure statement

The authors report there are no competing interests to declare.

References

- Advantage Engineering. 2021. *Water distribution pipe sizing*. Greenwood, IN: Advantage Engineering, Inc., FYI Document Library.
- AHRI. 2020. AHRI Standard 550/590 (I-P): 2020 standard for performance rating of water-chilling and heat pump water-heating packages using the vapor compression cycle. The Air-Conditioning, Heating, and Refrigeration Institute.
- ASHRAE. 2015. TC 9.9: Data center networking equipment—issues and best practices. The American Society of Heating, Refrigerating and Air-Conditioning Engineers.
- ASHRAE. 2021. ASHRAE guideline 36-2021—High-performance sequences of operation for HVAC systems. The American Society of Heating, Refrigerating and Air-Conditioning Engineers.
- BAC. 2013. Cooling tower pumping and piping. Baltimore Air Coil BAC Technical Resources.
- Belimo Aircontrols. 2021. *Electronic valve sizing and selection*. Technical documents. Danbury, CT: Belimo Aircontrols (USA), Inc.
- Blum, D., J. Arroyo, S. Huang, J. Drgoña, F. Jorissen, H. T. Walnut, Y. Chen, K. Benne, D. Vrabie, M. Wetter, et al. 2021. Building Optimization Testing Framework (BOPTTEST) for simulation-based benchmarking of control strategies in buildings. *Journal of Building Performance Simulation* 14 (5):586–610. [10.1080/19401493.2021.1986574](https://doi.org/10.1080/19401493.2021.1986574)
- Bortoff, S. A., P. Schwerdtner, C. Danielson, S. D. Cairano, and D. J. Burns. 2022. H-infinity loop-shaped model predictive control with HVAC application. *IEEE Transactions on Control Systems Technology* 30 (5):2188–203. [10.1109/TCST.2022.3141937](https://doi.org/10.1109/TCST.2022.3141937)
- Carrier Corporation. 2014. Product data: AquaForce 30XW150-400 water-cooled liquid screw chillers.
- Fan, C., K. Hinkelman, Y. Fu, W. Zuo, S. Huang, C. Shi, N. Mamaghani, C. Faulkner, and X. Zhou. 2021. Open-source modelica models for the control performance simulation of chiller plants with water-side economizer. *Applied Energy* 299:117337. [10.1016/j.apenergy.2021.117337](https://doi.org/10.1016/j.apenergy.2021.117337)
- Grahovac, M., P. Ehrlich, J. Hu, and M. Wetter. 2022, September. Data Center Chiller Plant: Simulation-based comparative control design case study. In *Proceedings of the 2022 Building Performance Analysis Conference and SimBuild, Chicago, IL*. [10.26868/25746308.2022.C042](https://doi.org/10.26868/25746308.2022.C042)
- Petschke, B. 2021. *AER—Eine neue Kennzahl für die Effizienz von Luftbewegung in Rechenzentren*. Hamburg, Germany: STULZ GMBH Newsroom.
- PG&E. 2012. Data Center Best Practices Guide: Energy efficiency solutions for high-performance data centers. Pacific Gas and Electric Company (PG&E).
- Rasmussen, N. 2007. *Calculating total cooling requirements for data centers*. Rueil-Malmaison, France: American Power Conversion.
- Shehabi, A., S. Smith, D. Sartor, R. Brown, and M. Herrlin. 2016. *United States Data Center energy usage report*. Berkeley, CA: Lawrence Berkeley National Laboratory, vol. LBNL-1005775.
- Taylor, S. 2014. How to design & control waterside economizers. *ASHRAE Journal* 56 (6):30–36.
- Trane. 2014. Chilled-water systems design issues. *Trane Engineers Newsletter* 43 (2):1–6.
- Trane. 2019. Selecting chilled-water coils for ASHRAE 90.1's New 15°F Delta T Requirement. *Trane Engineers Newsletter* 48 (2):1–8.
- Velimirovic, A. 2021. *Data center tiers explained*. phoenixNAP Global IT Services.
- Wetter, M. 2009. Modelica-based modelling and simulation to support research and development in building energy and control systems. *Journal of Building Performance Simulation* 2 (2):143–61. [10.1080/19401490902818259](https://doi.org/10.1080/19401490902818259)
- Wetter, M., P. Ehrlich, A. Gautier, M. Grahovac, P. Haves, J. Hu, A. Prakash, D. Robin, and K. Zhang. 2022. Open building control: Digitizing the control delivery from building energy modeling to specification, implementation and formal verification. *Energy* 238: 121501. [10.1016/j.energy.2021.121501](https://doi.org/10.1016/j.energy.2021.121501)
- Wetter, M., M. Grahovac, and J. Hu. 2018, August. Control description language. In 1st American Modelica Conference, 147–56. Cambridge, MA.
- Wetter, M., and J. Hu. 2019, March. *Quayside energy systems analysis*. Berkeley, CA: Lawrence Berkeley National Laboratory, vol. LBNL-2001197.
- Wetter, M., J. Hu, M. Grahovac, B. Eubanks, and P. Haves. 2018, September. OpenBuildingControl: Modeling feedback control as a step towards formal design, specification, deployment and verification of building control sequences. In *Proceedings of Building Performance Modeling Conference and SimBuild, 775–82*. Chicago, IL.
- Wetter, M., W. Zuo, T. S. Noudui, and X. Pang. 2014. Modelica buildings library. *Journal of Building Performance Simulation* 7 (4):253–70. [10.1080/19401493.2013.765506](https://doi.org/10.1080/19401493.2013.765506)
- Zhang, K., D. H. Blum, M. Grahovac, J. Hu, J. Granderson, and M. Wetter. 2020, March. Development and verification of control sequences for single-zone variable air volume system based on ASHRAE guideline 36. In *Proceedings of the American Modelica Conference, Boulder, CO*.

Appendix A. Closed-loop system models

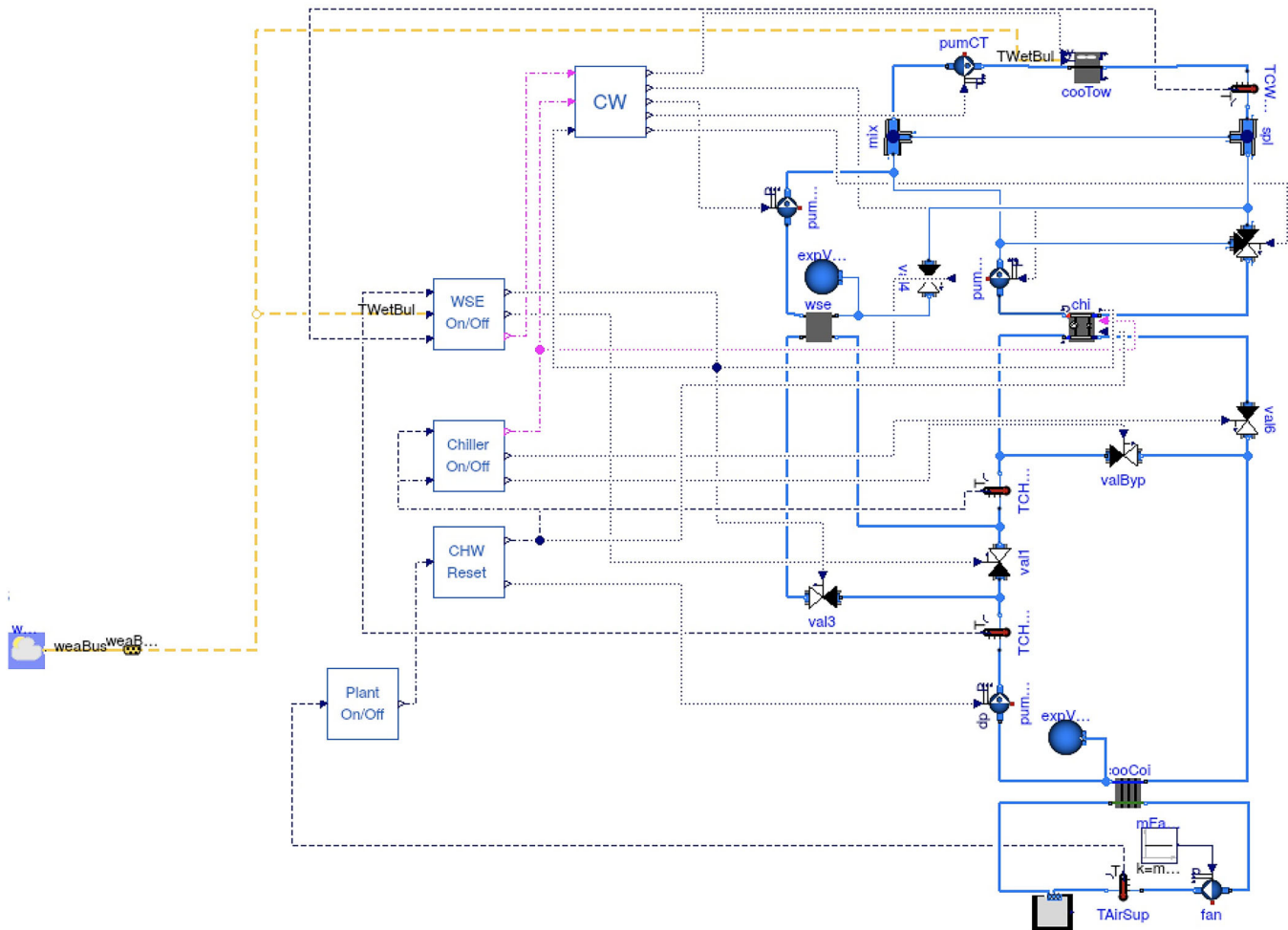


Fig. A1. Data center chiller plant graphical model with base controls. Left, connected with yellow dashed lines: weather data reader block. Middle, connected with dashed (sensor to controller signals), dash-dotted (controller to controller signals), and dotted (controller to actuator signals) lines: controller blocks. Right: chiller plant and data center zone blocks, from the bottom to the top: air loop including the data center zone, the cooling coil heat exchanger, the supply air fan, and the zone supply air temperature $T_{z,s}$ sensor; the CHW loop including the cooling coil heat exchanger, the CHW pump, the WSE heat exchanger, the chiller evaporator, bypass and isolation valves, and CHW return temperature sensors upstream and downstream of WSE, $T_{chw,r}$ and $T_{chw,r,d}$, respectively; and the CW loop including the chiller condenser, the outdoor side of the WSE heat exchanger, the CT, three CW-side pumps (serving the WSE, the chiller condenser, and the CT loops), the CW supply temperature $T_{cw,s}$ sensor, and the outdoor air wet-bulb temperature $T_{oa,w}$ sensor.

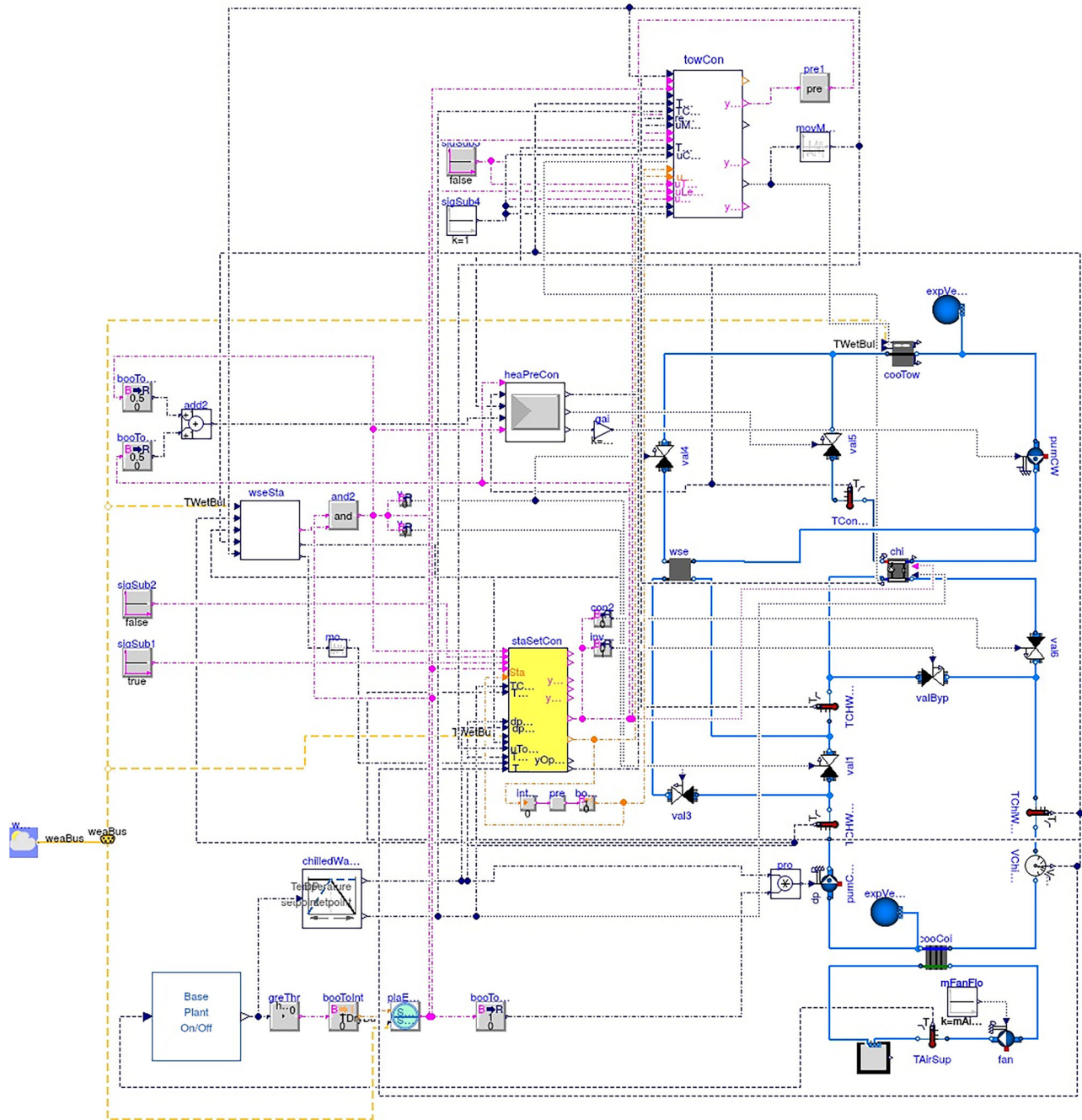


Fig. A2. Data center chiller plant graphical model with alternative controls based on ASHRAE Guideline 36. Left, connected with yellow dashed lines: weather data reader block. Middle, connected with dashed (sensor to controller signals), dash-dotted (controller to controller signals), and dotted (controller to actuator signals) lines: controller blocks. Right: chiller plant and data center zone blocks, from the bottom to the top: the air loop including the data center zone, the cooling coil heat exchanger, the supply air fan, and the zone supply air temperature $T_{z,s}$ sensor; the CHW loop including the cooling coil heat exchanger, the CHW pump, the WSE heat exchanger, the chiller evaporator, bypass and isolation valves, the CHW volume flow $\dot{V}_{chw,s}$ sensor, the CHW return temperature sensors upstream and downstream of WSE, $T_{chw,r}$ and $T_{chw,r,d}$, respectively, and the supply $T_{chw,s}$ temperature sensor; and the CW loop including the chiller condenser, the outdoor side of the WSE heat exchanger, the CT, the CW pump, the CW return temperature $T_{cw,r}$ sensor, and the outdoor air temperature T_{oa} sensor including the wet-bulb temperature $T_{oa,w}$ sensor.

Appendix B. Sizing parameters

Table B1. Selected sizing parameters.

Device	Parameter	Value and unit
Data center cooled zone	Total thermal output (IT loads and non-IT load apart from cooling)	500 kW
	Cold aisle supply air temperature set-point	27°C
	Cold aisle supply air temperature set-point low	25°C
	Cold aisle supply air temperature set-point high	29°C
Cooling coil	Air flow rate	33 kg/s
	Nominal temperature difference	15 K
	Pressure drop, air side	200 Pa
	Pressure drop, water side	24 kPa
Chiller	Nominal capacity	471 kW
	Temperature dead-band to enable	2.2 K
Chiller condenser	Pressure drop	42 kPa
Chiller evaporator	Pressure drop	19 kPa
CHW loop	Nominal temperature difference	10 K
	Temperature set-point limits	5.56 – 22°C
	Water flow rate	12 kg/s
	Differential pressure set-point limits	12,970 – 129,700 Pa
CW loop	Water flow rate	20 kg/s
Cooling tower	Height	1.5 m
	Pressure drop	15 kPa
	Approach temperature difference	4 K
	Nominal capacity	6.5 kW
Cooling tower fan	Pressure drop	6 kPa
Modulating control valve	Diameter	5 inches
	Total length	30 m
Pipes, CHW	Pressure drop ^a	4.5 kPa
	Diameter	6 inches
Pipes, CW	Total length	30 m
Pipes, CW, alternative case	Pressure drop ^a	4.3 kPa
Pipes, CW, alternative case	Total length	40 m
Pipes, CW, base case	Pressure drop ^a	5.7 kPa
WSE	Pressure drop, CW side	42 kPa
	Pressure drop, CHW side	15 kPa

^aAny modulation valve pressure drop is additional.

Appendix C. Energy use and PUE

Table C1. Per device and total annual and summer energy use for the base and the alternative case controllers.

Season	Controller	Device	Energy use in kWh at $T_{z,s, set}$:		
			27°C	29°C	25°C
Annual	Base case	Supply fan	99,021	99,021	99,021
		Cooling tower fan	56,938	56,938	56,938
		CHW pump	2,760	2,022	3,965
		CT pump	1,333	1,320	1,757
		WSE pump	15,382	15,382	15,378
		Total	175,615	174,682	183,488
	Alternative case	Supply fan	99,021	99,021	99,021
		Cooling tower fan	6,878	2,631	10,338
		CHW pump	7,582	7,346	8,169
		CW pump	17,211	17,070	24,095
Total		131,115	126,068	163,834	
Summer	Base case	Supply fan	25,773	25,773	25,773
		Cooling tower fan	14,820	14,820	14,820
		Chiller	156	0	5,598
		CHW pump	1,269	773	1,904
		CT pump	357	344	777
		WSE pump	4,003	4,003	3,999
		CW pump	26	1	796
		Total	46,404	45,713	53,666
	Alternative case	Supply fan	25,773	25,773	25,773
		Cooling tower fan	4,834	1,886	5,438
		Chiller	424	1	21,146
		CHW pump	2,151	1,926	2,570
		CW pump	4,584	4,443	11,110
		Total	37,766	34,028	66,036

Table C2. Per device and total annual and summer PUE for the base and the alternative case controllers. Per device PUE represents the participation of the device energy use in the data center PUE value. The device PUE divided by the data center PUE equals the device energy use divided by the total non-IT energy use including the cooling system.

Season	Controller	Device	PUE at $T_{z,s, set}$:		
			27°C	29°C	25°C
Annual	Base case	Supply fan	0.12	0.12	0.12
		Cooling tower fan	0.07	0.07	0.07
		CHW pump	0.00	0.00	0.00
		CT pump	0.00	0.00	0.00
		WSE pump	0.02	0.02	0.02
		Non-IT heat load	1.08	1.08	1.08
		Total	1.30	1.30	1.30
	Alternative case	Supply fan	0.13	0.13	0.12
		Cooling tower fan	0.01	0.00	0.01
		CHW pump	0.01	0.01	0.01
		CW pump	0.02	0.02	0.03
		Non-IT heat load	1.12	1.12	1.09
		Total	1.29	1.29	1.30

(Continued)

Table C2. (Continued).

Season	Controller	Device	PUE at $T_{z,s,set}$:		
			27°C	29°C	25°C
Summer	Base case	Supply fan	0.12	0.12	0.12
		Cooling tower fan	0.07	0.07	0.07
		CHW pump	0.01	0.00	0.01
		CT pump	0.00	0.00	0.00
		WSE pump	0.02	0.02	0.02
		CW pump	0.00	0.00	0.00
		Non-IT heat load	1.08	1.08	1.06
		Total	1.30	1.30	1.31
	Alternative case	Supply fan	0.13	0.13	0.12
		Cooling tower fan	0.02	0.01	0.02
		Chiller	0.00	0.00	0.10
		CHW pump	0.01	0.01	0.01
		CW pump	0.02	0.02	0.05
		Non-IT heat load	1.11	1.12	1.03
		Total	1.29	1.29	1.32